

Role of Concentration Level of the Nondiffusing Species in Turbulent Gas Phase Mass Transfer at Ordinary Mass Transfer Rates

DARSHANLAL T. WASAN and CHARLES R. WILKE

Lawrence Radiation Laboratory, University of California, Berkeley, California

Numerical solutions to the diffusion-convection equations are obtained with a digital computer to establish the role of concentration level of the nondiffusing species in nonequilibrium diffusion in fully developed turbulent flow of gases in pipes. Results indicate that under ordinary mass transfer rates for a system at constant Schmidt and Reynolds numbers product of the gas-phase mass transfer coefficient and the log mean partial pressure of the nondiffusing gas is nearly constant both in the mass transfer entry region and in the fully developed region. These results are compared with the experimental data on vaporization and absorption processes.

We show that the effect of the mass transfer section length on the rate of turbulent mass transfer is quite significant. Furthermore, the results of the diffusion-convection analysis are in better agreement with experimental data for sections of finite length than results calculated from the momentum-mass transfer analogy. The two methods agree in the limit for tubes of infinite length.

In many chemical engineering processes such as evaporation, humidification, partial condensation, absorption, and desorption the mass transfer process consists of the diffusion of a solute through a nondiffusing gas stream. The role of the concentration of the nondiffusing gas in the rate of transfer of solute by pure molecular diffusion has been well established by Stefan (16) and Maxwell (11) in the formulation of their classic diffusion equations. In recent years these equations were fully validated by experiments involving binary and ternary systems.

An interpretation of the Stefan-Maxwell diffusion equations for the case of diffusion of a solute through a stagnant gas implies that the diffusion flux established by a concentration gradient of the solute in the binary system creates a convective flow in the direction of the diffusion. The magnitude of the convective transport depends upon the concentration gradient of the solute and the concentration of the nondiffusing gas. In the interpretation of gas phase mass transfer processes by molecular diffusion through a hypothetical stagnant film, the convective transport resulting from the diffusion process has usually been accounted for through the film pressure factor. For diffusion of one gas through a second stagnant gas the film pressure factor becomes the log mean average partial pressure of the stagnant gas over the diffusion path, that is, p_{Bm} . The role of the film pressure factor has been well confirmed for pure molecular diffusion, but only in recent years attention has been focused on verifying its role for mass transfer in turbulent flow of gases as it occurs in absorption and vaporization processes.

Seshadri and Toor (14) have made an approximate theoretical analysis based on the analogy theory for $N_{Sc} = 1.0$ which indicates that the mass transfer coefficient varies inversely with p_{Bm} , in agreement with the film theory.

Cairns and Roper (2) were the first ones who deliber-

ately studied the influence of inert concentration level on the gas phase mass transfer coefficient. They evaporated water and condensed steam into air in a long wetted wall column similar to the one used by Gilliland and Sherwood (6). Cairns and Roper varied the p_{Bm}/P ratio from 0.15 to 0.97.

Further experimental study was undertaken by Westkaemper and White (24) who vaporized carbon tetrachloride into air from a pan mounted flush in the floor of a rectangular wind tunnel. The variation of p_{Bm}/P in their study was from 0.287 to 0.81.

The studies cited above have been in general, inconclusive and/or contradictory with regard to the effect of the film pressure factor. Much of the data scatter badly. This attests to the experimental difficulties involved in the accurate measurement of mass transfer rates and concentration differences over a wide range of inert gas composition in the various types of apparatus employed.

The most recent work on the investigation of the effect of concentration level upon the gas phase mass transfer coefficient was conducted by Behrmann (1) and recently reported by Vivian and Behrmann (17). In this study, ammonia was absorbed from gaseous streams of nitrogen and air into distilled water and aqueous ammonia solutions in a short wetted wall column. The mean inert mole fraction was varied over the range 0.934 to 0.058. Also desorption of ammonia from ammonia solution into air was studied. In this study variables of pressure and Schmidt and Reynolds numbers were held constant. The mass transfer Stanton number was correlated vs. mean inert mole fraction. Although considerable experimental scatter exists at low values of the mean inert mole fraction, the results of the absorption experiments were best correlated with the film pressure factor to the first power. However, the results of the data on desorption did not correlate with the absorption runs. Therefore, although this study appears to be best to date, the results show that the role of

Darshanlal T. Wasan is at the Illinois Institute of Technology, Chicago, Illinois.

the film pressure factor in desorption or vaporization processes can not be established with certainty.

A theoretical study of turbulent transport of mass into gaseous streams may be made through the solution of the diffusion convection equations. Considerable interest has been shown on the use of differential form of the rate equations for turbulent transport of heat and momentum. Recently, Kays (9) has summarized several of these studies. One of the earlier studies was made by Sleicher and Tribus (15) who presented solutions for the variation of the heat transfer coefficients in turbulent flow in pipes with a constant surface temperature and with no cross flow velocity. But as these authors pointed out, their solutions are not accurate for short transfer sections and for a gaseous range since more eigenvalues are needed than those presented in their paper. Furthermore, Kays (9) has recently pointed out that the Sleicher and Tribus results predict higher values for heat transfer coefficients for fully developed region in the gaseous range and therefore are not very accurate even for long transfer sections. This discrepancy is due to the eddy diffusivity distribution functions employed by these authors (15). Westkaemper and White (24) attempted numerical solutions to the diffusion convection equations for parallel plate geometry but they also neglected the cross flow velocity due to mass transfer. Their computed results did not agree with their measured mass transfer rates at low Reynolds number where the effect of the cross flow velocity was maximum.

The purpose of this work is to attempt numerical solutions of the diffusion convection equations for the case of convective mass transfer from a cylindrical tube into a turbulent gas in the presence of a finite cross flow velocity, and thus to establish theoretically the effect of the film pressure factor upon the transfer rates.

THEORETICAL ANALYSIS

The Equation of Convective Diffusion

Consider the case of vaporization of a liquid (or solid), A , from the wall of a tube over a mass transfer section of finite length, Z_L , into which a binary mixture consisting of varying amounts of diffusing species, A , and inert gas, B , enters with a fully developed velocity distribution as shown in Figure 1. Component A is maintained at a constant concentration (vapor pressure) at the wall over the entire section. The mass transfer occurs by diffusion and also by bulk transport of material by a velocity in the radial direction. The following assumptions are made:

1. $\partial C_A / \partial \theta = 0$, that is, diffusion in θ direction is negligible.
2. $\partial U / \partial z = 0$, that is, fluid enters the tube with a fully developed velocity profile and under ordinary mass transfer rates the contribution of the mass transfer to the mean velocity is negligible. This assumption is verified by the experimental study recently completed (22).
3. The $\partial / \partial z [(D + E) \partial C_A / \partial z]$ term which represents diffusion in the axial direction is negligible. Schneider's (13) theoretical analysis seems to support this assumption.
4. An eddy diffusivity based on the mole average velocity is taken to be equal to the eddy diffusivity based on

the mass average velocity. At low mass transfer rates this assumption appears to be satisfactory. In the subsequent treatment therefore, a single eddy diffusivity E will be designated for both cases.

This results in the following simplified form of the equation of convective diffusion:

$$V_z \frac{\partial C_A}{\partial r} + V_r \frac{\partial C_A}{\partial z} = \frac{1}{r} \frac{\partial}{\partial r} \left[(D + E) r \frac{\partial C_A}{\partial r} \right] \quad (1)$$

Diffusion of Solute Through an Inert Gas

It is often noted that in many mass transfer processes, such as evaporation or absorption of solute in gaseous streams, the transfer mechanism can be approximated as that of diffusion of solute through a gas which exhibits no net transfer in the direction of the solute transfer. Therefore, in this case the rate equation at the boundary of the transfer, at the pipe wall, becomes

$$N_B = - (D + E) \frac{\partial C_B}{\partial r} + V_r C_B = 0 \quad (2)$$

Strictly speaking the net mass flux of component B is zero only at the wall since the wall is impermeable to B . But in this work we shall assume that at ordinary mass transfer rates the condition, $N_B = 0$, is true at every radial position in the pipe. Then from Equation (2) one obtains the relationship between the cross flow velocity distribution and the concentration gradient as follows:

$$V_r = - \frac{(D + E)}{C_t - C_A} \frac{\partial C_A}{\partial r} \quad (3)$$

It is noted that the cross flow velocity is zero at the axis of the pipe since the concentration gradient is zero and cross flow velocity is maximum at the pipe wall.

Since we are dealing with diffusion processes in gaseous streams it is convenient to use partial pressure instead of molar concentrations as a driving force. By assuming an ideal gas law for the binary solute-inert mixture the following relationships result in terms of partial pressure driving force:

$$N_A = - \left[\frac{(D + E)}{R'T} \frac{\partial p_A}{\partial r} + \frac{(D + E)}{(P - p_A)} \frac{p_A}{R'T} \frac{\partial p_A}{\partial r} \right] \quad (4)$$

and the diffusion convection Equation (1) can be written as

$$\begin{aligned} V_z \frac{\partial p_A}{\partial z} &= [D + E(r)] \frac{\partial^2 p_A}{\partial r^2} + \left[\frac{D + E(r)}{r} + \frac{\partial E(r)}{\partial r} \right] \frac{\partial p_A}{\partial r} \\ &\quad + \left[\frac{D + E(r)}{P - p_A} \right] \left(\frac{\partial p_A}{\partial r} \right)^2 \end{aligned} \quad (5)$$

This equation forms the basis for the theoretical consideration of transfer of one component into a turbulent solute-inert binary gas stream. In order to complete the mathematical formulation of this problem the boundary conditions of the system should be considered as discussed in the following section.

Boundary Conditions

The boundary values of the system are as follows:

1. The concentration at the wall is constant for all downstream distance z . Hence $p_A = p_{AW}$, at $r = R$ and for all z .
2. The concentration of the inlet gas is constant and

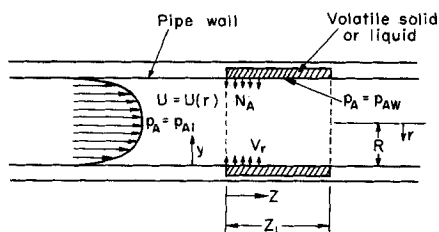


Fig. 1. Schematic diagram of the diffusion convection model.

$p_A = p_{Ai}$, at $z = 0$ and for all $r > 0$.

3. There is no concentration gradient at the axis of the tube. Hence concentration profile is symmetric around the radial axis. That is $\partial p_A / \partial r = 0$, at $r = 0$ and for all z .

It is evident that the basic problem is the determination of the concentration distribution as a function of radial and axial positions. This involves the simultaneous solution of the equations of change. But the mathematical nature of these equations does not permit a rigorous solution in all but a few simplified cases. For the specific problem at hand a numerical solution of the diffusion convection equation is sought.

Eddy Diffusivity and Mean Velocity Distributions

It is appropriate now to consider the diffusion convection Equation (5) since it expresses the relationship between the concentration gradients in the radial and the axial positions in the system. Equation (5) may be solved if the variation of the time averaged velocity, V_z , and the variation of the eddy diffusivity, E , with the positions in the system are known. A basic uncertainty in the theoretical treatment of a turbulent mass transfer process lies in not knowing these distribution functions under the conditions of finite mass exchange between the fluid streams and the pipe wall. In the absence of such information concerning the eddy distribution in the past, several analyses had assumed that under low mass transfer rates E is the same for both the momentum and the mass transfer process, at least in the region close to the wall where most of the transfer takes place. This resulted in several empirical expressions having been proposed for the eddy viscosity distributions in the vicinity of a pipe wall. But as we pointed out earlier, the real success of any analysis depends to a considerable extent on how carefully the eddy variation is chosen near to the wall.

It is considered here that the choice of the assumed eddy distribution will be justified only if it satisfies the equations of mean motion; it is continuous with respect to that obtained from von Karman's logarithmic distribution in the turbulent core region; it is compatible with the mean velocity distribution expression, and gives no discontinuity in the velocity distribution function over the region from the wall to the point away from the wall beyond which E is assumed constant; it eliminates the concept of sharply defined fluid layers and describes the whole wall region where mass transfer mainly takes place; and it agrees with the experimental data. All these criteria except the first criterion have been recently set by Gowariker (7, 8).

Using the equations of continuity and the equations of mean motion we have derived (20) compatible expressions for velocity and eddy viscosity distributions for the whole wall region of the fully developed turbulent pipe flow. Our proposed expressions agree with the experimental data on velocity and eddy variations. Furthermore, using these distributions we have presented (21) the momentum-mass transfer analogy expressions and found an excellent agreement with the experimental data on mass and heat transfer rates. Since the present eddy and mean velocity distributions satisfy all the criteria set in the previous paragraph for the purpose of solving the diffusion convection Equation (5), these distributions will be chosen for the wall region where mass transfer mainly takes place. These velocity and eddy-viscosity distributions for the wall region are given as follows:

$$U^+ = y^+ - 1.04 \times 10^{-4} (y^+)^4 + 3.03 \times 10^{-6} (y^+)^5, \quad \text{for } 0 \leq y^+ \leq 20 \quad (6)$$

$$\frac{\epsilon}{\nu} = \frac{4.16 \times 10^{-4} (y^+)^3 - 15.15 \times 10^{-6} (y^+)^4}{1 - 4.16 \times 10^{-4} (y^+)^3 + 15.15 \times 10^{-6} (y^+)^4},$$

$$\text{for } 0 \leq y^+ \leq 20 \quad (7)$$

Where U^+ and y^+ are the dimensionless velocity and dimensionless distance from the wall.*

In order to obtain these distributions in the wall region we have used von Karman's logarithmic velocity distribution (18) for the fully developed turbulent core region. In the present analysis von Karman's velocity expression will be retained for the region away from the wall. Von Karman's velocity expression is written

$$U^+ = 2.5 \ln y^+ + 5.5 \text{ for } y^+ \geq 20 \quad (8)$$

For steady flow in a cylindrical tube, the shear stress is proportional to the distance from the axis and the eddy viscosity function for the region away from the wall is obtained from von Karman's velocity distribution function:

$$\frac{\epsilon}{\nu} = \frac{y^+ (1 - y/R)}{2.5} - 1 \quad (9)$$

In the past (10) it has been observed experimentally that the eddy viscosity goes through a maximum and reaches a constant value at the axis of a tube. Therefore for the purpose of present analysis we shall assume the variation of the eddy viscosity function as given by the relationship (9) to a distance, y_1 , far away from the wall and a constant value of the eddy viscosity that is assumed from there on to the axis. The point y_1 beyond which the value of eddy viscosity is assumed constant is determined by the following analysis.

Consider constant eddy diffusivity for momentum in the turbulent core of the turbulent velocity field. With this assumption the integration of the equation for turbulent shear stress between the point y_1 and the central axis gives

$$(U_{\max} - U_1) = \frac{\tau_0 g_c}{E' 2R} (y_1 - R)^2 = \frac{\tau_0 g_c}{2E'} (r_1/R)^2 \cdot R \quad (10)$$

Where $E' = \mu + \rho E$; U_1 corresponds to the velocity at the point y_1 ; U_{\max} corresponds to the velocity at the central axis of the pipe and τ_0 is defined as

$$g_c \tau_0 = U^{*2} \rho$$

Then relation (10) can be rewritten as

$$\frac{(U_{\max} - U_1)}{U^*} = \frac{U^* R \rho}{2E'} (r_1/R)^2 \quad (11)$$

Thus if a plot of $U_{\max} - U/U^*$ vs. r^2 is prepared from the experimental data on the fully developed velocity profile, the slope of the straight line through the data would be directly related to the constant total viscosity $E + \mu$. This technique of determining E has been previously used by Clauser (3). A plot of $U_{\max} - U/U^*$ vs. y/R of the experimental velocity distribution data for all Reynolds numbers is given by Schlichting (12). When Equation (11) is used in conjunction with the plot given by Schlichting, the point of junction y_1 is found where the values of eddy viscosity given by Equation (11) and by the von Karman relation [Equation (9)] approximately agree. This point of junction was found to be at about 30% of the distance away from the wall, that is $y_1/R = 0.3$.

It should be pointed out that the present theoretical results for mass transfer are found to be rather insensitive to small errors in the choice of the junction point.

Once the value of the junction point has been deter-

* The precise intersection of Equations (6) and (8) occurs at $y^+ = 19.75$. Use of the rounded off value of 20 has negligible effect on the present calculations or the earlier analogy application (21).

mined then the averaged value of the eddy viscosity which represents the central turbulent core can be obtained over a wide range of Reynolds number by the relationship (11) as follows:

$$\frac{E'}{U^* R} = \frac{\mu/\rho + E}{U^* R} \approx 8.2 \times 10^{-2} \quad (12)$$

This expression for eddy viscosity is similar to the result of Clauser (3) in the turbulent boundary layer.

Nondimensionalized Equations

Since dimensionless velocity U^+ , in the previous section, is given as the function of the dimensionless distance y^+ it is convenient to nondimensionalize the diffusion convection equation and the boundary conditions of the system. Using a nondimensionalizing procedure the diffusion convection Equation (5) becomes:

$$\frac{\partial p_A}{\partial Z} = \left(\frac{4}{N_{Re}} \frac{1}{\sqrt{f/2}} \frac{Z_L}{d} \frac{1}{U^+} \right) \left[\left(\frac{1}{N_{Sc}} + E(y^*) \right) \frac{\partial^2 p_A}{\partial y^{*2}} - \left(\frac{1/N_{Sc} + E(y^*)}{1 - y^*} - \frac{\partial E}{\partial y^*} \right) \frac{\partial p_A}{\partial y^*} + \left(\frac{1/N_{Sc} + E(y^*)}{\frac{P - p_{Ai}}{P_{AW} - p_{Ai}} - p_A} \right) \left(\frac{\partial p_A}{\partial y^*} \right)^2 \right] \quad (13)$$

The boundary values of the system when expressed in dimensionless form become:

1. $p_A = 1$ at $y^* = 0$ for all Z
2. $p_A = 0$ at $Z = 0$ for all $y^* > 0$
3. $\frac{\partial p_A}{\partial y^*} = 0$ at $y^* = 1$ for all Z

In this nondimensionalizing procedure an explicit influence of Reynolds number is noted. As Reynolds number becomes large the concentration gradient in the axial direction becomes small, and in the limit the concentration gradient approaches zero.

As we pointed out earlier it is not possible to obtain an analytical solution of the diffusion convection equations. Therefore in order to accomplish an accurate solution of the diffusion convection equations which will satisfy the given boundary conditions a numerical approach is adopted. The method used to solve the diffusion convection equations consists of finite difference technique. A four point explicit method of finite differences is used. IBM 7090 and IBM 7094 digital computers were employed to solve the equations. Details of the procedure and the computer program are available elsewhere (19).

NUMERICAL RESULTS

Sufficiently small increments were obtained by dividing the radial distance into twenty divisions near the wall between $y^* = 0$ and $y^* = 0.2$ and five divisions from that point to the radius. The longitudinal distance Z consisted of 10,000 increments. The grid size was developed by stability tests in which successively smaller grids were used until the numerical results no longer changed. For each run there were 250,000 ($10,000 \times 25$) values of concentration calculated and it was not practical to print out all this information. Therefore only 500, (20×25), values of concentration were saved at twenty equally spaced increments of $\Delta Z = 0.05$.

From calculated concentration profiles the cup-mixed averaged value of the concentration $p_{A_{avg}}$ was calculated for every incremental value of Z where $p_{A_{avg}}$ is the mean concentration over a cross section and is defined by

$$p_{A_{avg}} = \frac{\int_0^1 (1 - y^*) U^+(y^*) p_A(y^*) dy^*}{\int_0^1 (1 - y^*) U^+(y^*) dy^*} \quad (14)$$

From the concentration profiles the concentration gradients were computed and the mass flux at the wall for every incremental value of Z was then calculated by the relation

$$(N_{AW})_Z = 2 \frac{p_{AW} - p_{Ai}}{P - p_{Ai}} \frac{PD}{RTd} \left(\frac{\partial p_A}{\partial y^*} \right)_w \quad (15)$$

Since the computation of the local mass fluxes involves the knowledge of the concentration gradient which cannot be determined with very great precision, the local mass transfer rates were also computed and compared with the following relation

$$(N_{AW})_Z = \frac{p_{AW} - p_{Ai}}{2RT} \frac{\nu}{Z_L} N_{Re} \sqrt{f/2} \frac{d}{dz} \int_0^1 (1 - y^*) U^+(y^*) p_A(y^*) dy^* \quad (16)$$

The above relation can be derived by a mass balance over a cylindrical slice. This equation permits the calculation of N_A first, by a graphical integration which is a smoothing effect, then a differentiation. This method of calculating mass fluxes was chosen in this study.

TABLE 1. GILLILAND-SHERWOOD VAPORIZATION DATA

System:		Air-n Butyl alcohol	
$N_{Re}^* = 4,150;$		$N_{Sc} = 1.88$	
$Z_L = 117 \text{ cm.};$		$d = 2.67 \text{ cm.}$	
$T_L = 50^\circ \text{C.};$		$p_v = 38 \text{ mm. mercury}$	
		$p_{Ai} = 0$	
Measured values		Predicted values	Analogy theory prediction
Exit conc. 17.5 mm. mercury		14.5 mm. mercury	—
N_{St} 0.00401		0.00372	0.00312

* Reynolds numbers are based on gas velocities relative to the pipe wall.

TABLE 2. CAIRNS-ROPER VAPORIZATION DATA

System:		Air-water	
$N_{Re}^* = 8,925;$		$N_{Sc} = 0.60$	
$Z_L = 94.62 \text{ cm.};$		$d = 2.29 \text{ cm.}$	
$T_L = 32^\circ \text{C.};$		$p_v = 35.9 \text{ mm. mercury}$	
Measured values		Predicted values	Analogy theory prediction
Exit conc. 23.52 mm. mercury		24.46 mm. mercury	—
N_{St} 0.0058		0.0059	0.0054

* Reynolds numbers are based on gas velocities relative to the pipe wall.

From the knowledge of the mass fluxes and the average concentration, the mass transfer coefficient, k_g , was computed for every incremental value of Z , where k_g is defined by

$$(N_{AW})_Z = k_g (p_{AW} - p_{A_{avg}}) \quad (17)$$

From these calculations Sherwood and Stanton numbers were computed. The local Sherwood number is defined as:

$$N_{Sh} = \frac{k_g R T d}{D} = \frac{2P(p_{AW} - p_{Ai})}{(P - p_{AW})(p_{AW} - p_{A_{avg}})} \left(\frac{\partial p_A}{\partial y^*} \right)_w \quad (18)$$

and Stanton number (with the film pressure factor included) as:

$$N_{St} = \frac{k_c}{U_0} \frac{P_{BM}}{P} = \frac{P_{BM}}{P} N_{Sh}/N_{Re} \cdot N_{Sc} \\ = \frac{k_g R T P_{BM}}{G P} = \frac{k_c}{U_0} x_f \quad (19)$$

As a test of the calculation method and the assumptions, a number of Gilliland and Sherwood's (6), and Cairns and Roper's (2) wetted wall columns experiments was simulated on the computer. Two of these results are given in Table 1. Values of the calculated exit concentration and the log mean Stanton number are compared with the experimental values of Gilliland and Sherwood. The calculated Stanton number is also compared with the one calculated from the analogy theory of the authors (21). In Table 2 a similar comparison is made with the Cairns and Roper experimental value. It is seen that in these two cases and the others tested, the calculated values give better results than the analogy calculation.

Having established some confidence in the method, hypothetical cases were studied. Concentration profiles and local Stanton numbers were computed over a range of values of Z , Schmidt number and Reynolds number. In the test system the driving force, $(p_{AW} - p_{Ai})$, was set at 10 mm. and the inlet condition at 1 atm. total pressure. Calculated quantities are tabulated elsewhere (19).

Figure 2 shows the variation in local Stanton number for a hypothetical system with $N_{Sc} = 1$. At a Z_L/d of about 18 the Stanton number approaches a constant value. The average Stanton number based on a log mean driving force over the entire section is shown by the single point at $Z_L/d \approx 18$. It should be pointed out that the diffusion convection result approaches satisfactorily in the limit, the value obtained from the analogy consideration of momentum, mass, or heat transfer in pipes. The analogy result, as shown by the dashed line, is the one calculated from the analogy expression recently proposed by the authors (21) which is known to fit the experimental data on mass and heat transfer.

Figure 3 shows the calculation similar to the preceding one for a system with $N_{Sc} = 2.5$. Again, the diffusion convection calculation seems satisfactory. It is of interest

that in both cases considered, even for a test section of 18 diam. length, the log and distance mean Stanton numbers are significantly higher than the terminal local values. This substantial effect of test section length may account for some of the disagreement among various experimental studies in which a constant Stanton number was assumed.

From foregoing comparisons of the numerical solution of the diffusion convection equation with several experimental results it can be concluded that the numerical procedure and the assumptions involved are satisfactory.

In order to establish the role of film pressure factor in gas phase turbulent mass transport processes, several vaporization experiments were simulated in which film pressure factor (x_f or y_{BM}) was varied over a wide range of Schmidt number, the length of the transfer section and the Reynolds number. Figure 4 shows our computer results at $N_{Re} = 10,000$ in a pipe of 17.7 diam. length and for the values of Schmidt number varying from $N_{Sc} = 0.2$ to $N_{Sc} = 2.5$. Results show that within the limit of the calculation error the log mean Stanton number is constant over a wide range of x_f , thus indicating that the film pressure factor enters to the first power.

In order to establish the role of film pressure factor in the mass transfer entry region, typical vaporization experiments for a case of Z_L/d of 2 were simulated on the computer. These results are shown in Figure 5. Again it is seen that within the limit of the calculation error, film pressure enters to the first power.

It is of interest to compare our diffusion convection results with those of Behrmann's (1) experimental data. One of Behrmann's experimental runs on desorption of ammonia from ammonia solution into air is simulated on the computer and x_f is varied over a wide range at $N_{Sc} = 0.675$. Figure 6 compares our results with those of Behrmann's experimental data on absorption. It is of interest that the best curve through our calculated points agrees well with the least squares line representing Behrmann's data. Since our diffusion convection results agree with the absorption data reported by Behrmann, it may be concluded that the direction of mass transfer does not influence the mass transfer coefficient, and hence it may be generally concluded that the mass transfer coefficient varies inversely with the film pressure to the first power in absorption, desorption, or vaporization processes occurring in fully developed turbulent flow of gases in pipes.

DISCUSSION

From the preceding numerical results it may be concluded that, for practical purposes, the role of the concentration level of nondiffusing gases in turbulent transport is the same as that in pure molecular diffusion processes. But despite these conclusions there exists a number of inherent limitations and uncertainties concerning its true role in the gas phase turbulent mass transfer process. A major uncertainty concerning the validity of one of the

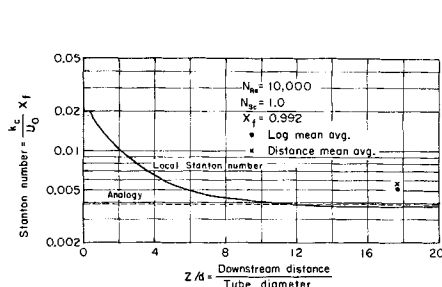


Fig. 2. Variation of Stanton number with downstream distance at $N_{Sc} = 1.0$.

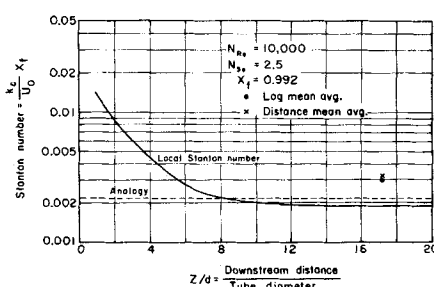


Fig. 3. Variation of Stanton number with downstream distance at $N_{Sc} = 2.5$.

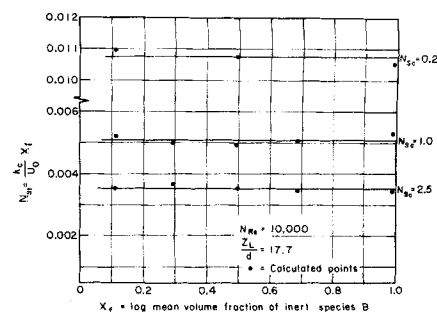


Fig. 4. Effect of inert gas concentration on transfer coefficient for $Z_L/d = 17.7$.

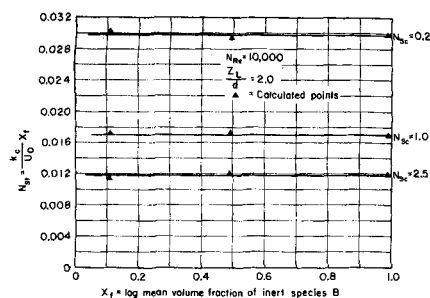


Fig. 5. Effect of inert gas concentration on transfer coefficient for $Z_L/d = 2.0$.

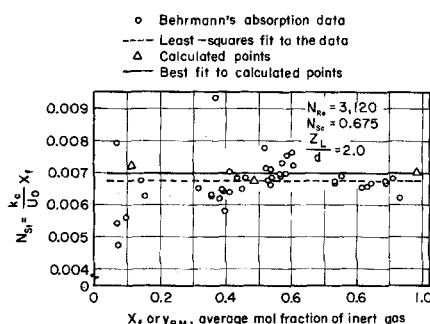


Fig. 6. Comparison of present theory with Behrmann's experimental data.

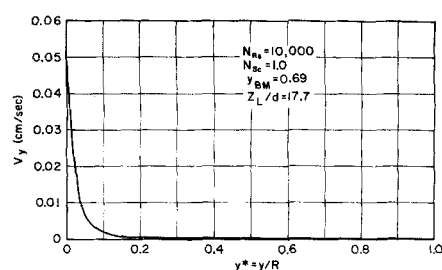


Fig. 7. Variation of radial velocity with the distance.

basic assumptions made in this development will be discussed first.

In the diffusion convection analysis it is assumed that the net radial flux of nondiffusing species vanishes everywhere in the diffusion system. However, as pointed out in the previous sections, this condition is satisfied only at the solid boundary. In order to check the validity of this assumption local values of mass transfer rates of nondiffusing species are estimated from the knowledge of the calculated radial concentration profiles. The results of a typical vaporization case are tabulated in Table 3. In view of the extremely small magnitude of N_B , in com-

TABLE 3. CALCULATED RADIAL VARIATION IN MASS FLUX OF STAGNANT COMPONENT B.

$N_{Sc} = 1.0,$ y/r	$y_{Bm} = 0.69,$ N_B	$N_{Re} = 10,000,$ $Z/d = 17.7$ $N_B/N_B + N_A$
0	0	0
0.01	2×10^{-10}	1.3×10^{-4}
0.02	3.7×10^{-10}	2.5×10^{-4}
0.03	4.3×10^{-10}	2.9×10^{-4}
0.04	5.1×10^{-10}	3.4×10^{-4}
0.05	7.1×10^{-10}	4.7×10^{-4}
0.1	5.4×10^{-10}	3.6×10^{-4}
0.2	4.8×10^{-10}	3.2×10^{-4}
0.4	1.1×10^{-10}	7.1×10^{-5}
0.6	3.7×10^{-11}	2.5×10^{-5}
1.0	0	—

parison to the total mass flux, it may be reasonably assumed that species B is stagnant.

To gain some further insight into the case of stagnant B diffusion, we may examine the typical magnitude of the interfacial velocity resulting from the diffusion flux. Figure 7 shows a typical variation of radial velocity component calculated from Equation (3) by using the computed concentration profiles. The shape of the curve suggests that the radial velocity component decays quite rapidly with distance from the wall under low mass transfer rates. Therefore in view of the small values of radial velocities it is not surprising to find that the calculated ratio of flux of B to the total flux is small.

Besides the major assumption of stagnant B diffusion there are inherent limitations in the present analysis. Examination of Equation (18), which relates the mass transfer coefficient to the concentration gradient and the bulk averaged concentration, reveals that in the special case of diffusion of A through a stagnant B the local mass transfer coefficient can be related to the concentrations of B as follows:

$$k_y \propto \left(\frac{1}{y_{BW}} \right) \left(\frac{y_{BW} - y_{Bi}}{y_{BW} - y_{Bavg}} \right) \left(\frac{\partial y_B}{\partial y^*} \right)_w \quad (20)$$

where

$k_y = N_A/y_{AW} - y_{Aavg}$ = mass transfer coefficient based on mole fraction differences

and

$$y_B = \frac{y_B - y_{Bi}}{y_{BW} - y_{Bi}}.$$

It is noted that in this formulation the local mass transfer coefficient appears to vary with the local concentration gradient of B at the wall, the mole fraction of B at the wall and the ratio of the concentration differences of the nondiffusing species, between the value at the phase boundary and the incoming stream, and between the phase boundary and the local averaged value. It should be pointed out that variation of the gas phase mass transfer coefficient with the film pressure factor is not explicit in the formulation.

In the study of nonequivalence diffusion in laminar boundary layer flows, it is observed (5, 6) that the mass transfer coefficient varies directly with the concentration gradient at the phase boundary and inversely with the concentration of the nondiffusing species at the phase boundary. In arriving at these results it is usually assumed that the averaged concentration can be fixed arbitrarily as an inlet concentration. This appears to be a reasonable assumption in liquid systems. Since, in gas phase transfer in fully developed turbulent pipe flow the concentration gradient, as well as the averaged concentration of the nondiffusing species, may vary locally, y_{BW} does not necessarily enter in the same manner as in the laminar boundary layer case.

It should be pointed out that in the case of low concentration differences in species A between the wall and the bulk stream (which is the case under consideration) local values of the film pressure factor do not differ greatly from the values of the concentration of the nondiffusing species at the phase boundary. It is of interest to note also that in all hypothetical cases considered here, the values of y_{BM} did not differ by more than 3% from the corresponding values of y_{BW} . Therefore it may be concluded that under conditions normally encountered in the design of mass transfer equipment the choice of y_{BM} appears satisfactory.

In the case of very high mass transfer rates the velocity field may be appreciably affected by the diffusion flux. Therefore, knowledge of the variations of the eddy diffusion coefficients and the velocity with position in the pipe under finite mass transfer rates is essential before the diffusion convection calculations can be carried out. Therefore the role of the concentration level of the nondiffusing species in the gas phase transport processes under very high mass transfer rates is still undetermined. However, the method of calculations presented in this study should prove to be valid in the range of mass transfer rates normally encountered in separation processes.

CONCLUSIONS

1. From the results of this investigation it may be concluded that under low mass transfer rates for a system at constant Schmidt and Reynolds number in fully developed

turbulent flow of gases in pipes, the product of the gas phase mass transfer coefficient and the log-mean mole fraction of the nondiffusing gas is nearly constant both in the mass transfer entry region and in the fully developed regions.

2. Mass transfer rates predicted by our diffusion convection calculations for desorption agree quite well with Behrmann's absorption data. Hence it may be concluded that there is no effect of the direction of the mass transfer on the mass transfer coefficient.

3. We show that the effect of the mass transfer section length on the rate of mass transfer is generally quite significant, and the results of the diffusion convection analysis for long mass transfer sections approach the momentum and mass transfer analogy result satisfactorily in the limit.

4. We show that close agreement between the predicted values and the experimental data of mass transfer rates supports the use of our velocity distribution function and assumed equality of the eddy diffusivities for momentum and mass.

ACKNOWLEDGMENT

The authors are grateful to Professor D. R. Olander who offered many valuable suggestions during the course of this investigation. This work was performed under the auspices of the U. S. Atomic Energy Commission.

NOTATION

A = diffusing species
 B = stagnant species
 C_A = molar concentration of species A
 C_{AW} = molar concentration of species A at the wall
 C_{avg} = averaged molar concentration of species A
 C_B = molar concentration of species B
 C_i = molar concentration of species i
 C_t = total molar concentration
 d = diameter of a pipe
 D = molecular diffusivity
 E = eddy diffusivity
 E = E/ν
 f = friction factor
 g_c = conversion constant
 k_c = mass transfer coefficient based on molar concentration difference
 k_g = gas phase mass transfer coefficient based on partial pressure difference
 k_y = gas phase mass transfer coefficient based on mole fraction difference
 N_A = molar flux of species A
 N_{AW} = molar flux of species A at the wall
 N_B = molar flux of species B
 P = total pressure
 P_A = partial pressure of species A
 $P_A = \frac{p_A - p_{Ai}}{p_{AW} - p_{Ai}}$
 p_{Ai} = partial pressure of species A in the inlet
 p_{avg} = averaged partial pressure of species A
 p_{AW} = partial pressure of species A at the wall
 p_B = partial pressure of species B
 p_{BW} = partial pressure of species B at the wall
 p_{BM} = log mean partial pressure of species B
 r = radial distance
 R = radius of pipe
 R' = gas constant
 T = temperature
 $U^* = \sqrt{\tau_0 g_c / \rho} = \sqrt{\frac{f}{2}} \cdot U_0$
 U = time-averaged mass velocity in axial direction

U_{max} = maximum velocity
 U_0 = averaged velocity
 V_r = radial velocity
 V_z = time-averaged molar velocity in Z direction
 X_f = film pressure factor
 y^+ = yU^*/ν
 y_B = mole fraction of inert component B
 y_{BM} = log mean mole fraction of inert component B
 y^* = y/R
 y_{BW} = mole fraction of inert component B at the wall
 Z = axial direction
 Z_L = length of pipe
 $Z = Z/Z_L$

Greek Letters

ρ = density
 μ = viscosity
 ν = kinematic viscosity
 ϵ = eddy viscosity
 θ = azimuthal direction
 τ = shear stress
 τ_0 = shear stress at the wall

Dimensionless Groups

N_{Re} = Reynolds number, $U_0 d / \nu$
 N_{Sc} = Schmidt number, ν / D
 N_{Sh} = Sherwood number, $k_g R' T d / D$
 N_{St} = Stanton number, $k_c X_f / U_0$

LITERATURE CITED

- Behrmann, W. C., Ph.D. thesis Mass. Inst. Tech., (1960).
- Cairns, R. C., and G. H. Roper, *Chem. Eng. Sci.*, **3**, 97 (1954).
- Clauser, F. H., "Advances in Applied Mechanics," Vol. IV, Academic Press, New York (1956).
- Emanuel, A., Ph.D. thesis, Univer. California, Berkeley (1962).
- , and D. R. Olander, *Int. J. Heat Mass Transfer* **7**, 539 (1964).
- Gilliland, E. R., and T. K. Sherwood, *Ind. Eng. Chem.* **26**, 516 (1934).
- Gowariker, V. R., U. K. A. Energy Authority, AERE-1055 (1962).
- Ibid., AERE-M086 (1962).
- Kays, W. M., "Convective Heat and Mass Transfer," McGraw-Hill, New York, pp. 186, 188 (1966).
- Lynn, S., *AIChE J.*, **5**, 566 (1959).
- Maxwell, J. C., *Phil. Trans. Roy. Soc. London, Ser. A.*, **157**, 49 (1867).
- Schlichting, H., "Boundary Layer Theory," McGraw-Hill, New York (1960).
- Schneider, P. J., *Trans. Am. Soc. Mech. Engrs.* **79**, 765 (1957).
- Seshadri, C. V., and H. L. Toor, *Indian Chem. Eng.* **95**, (1963).
- Sleicher, C. A., and M. Tribus, "Heat Transfer and Fluid Mechanics Institute," p. 59, Stanford Univer. Press, (1956).
- Stefan, J., *Stizher-Akad. Wiss. Wien, Math-Natur.* **k1**, 63 Abt II (1871).
- Vivian, J. E., and W. C. Behrmann, *AIChE J.* **11**, 656 (1965).
- von Karman, T., *Trans. Am. Soc. Mech. Engrs.* **61**, 705 (1939).
- Wasan, D. T., and C. R. Wilke, Lawrence Radiation Lab. Rept. UCRL-16221 (January 1965).
- , C. L. Tien, and C. R. Wilke, *AIChE J.* **9**, 567 (1963).
- , and C. R. Wilke, *Int. J. Heat Mass Transfer* **7**, 87 (1964).
- , R. M. Davis, and C. R. Wilke, *AIChE J.*, **14**, 227 (1968).
- , T. K. Subramaniam, and S. S. Randhava, *Chem. Eng.*, 165 (Feb., 1966).
- Westkaemper, L. E., and R. R. White, *AIChE J.* **3**, 69 (1957).

Manuscript received April 22, 1966; revision received September 26, 1967; paper accepted September 28, 1967.